Transient currents and universal time scales for a fully time-dependent quantum dot in the Kondo regime

Martin Plihal and David C. Langreth
Center for Materials Theory, Department of Physics and Astronomy, Rutgers University, Piscataway, New Jersey 08854-8019, USA

Peter Nordlander
Department of Physics and Rice Quantum Institute, Rice University, Houston, Texas 77251-1892, USA
(Received 28 September 2004; revised manuscript received 18 January 2005; published 25 April 2005)

Using the time-dependent noncrossing approximation, we calculate the transient response of the current through a quantum dot subject to a finite bias when the dot level is moved suddenly into a regime where the Kondo effect is present. After an initial small but rapid response, the time-dependent conductance is a universal function of the temperature, bias, and inverse time, all expressed in units of the Kondo temperature. Two timescales emerge: the first is the time to reach a quasimetastable point where the Kondo resonance is formed as a broad structure of half-width of the order of the bias; the second is the longer time required for the narrower split peak structure to emerge from the previous structure and to become fully formed. The first time can be measured by the gross risetime of the conductance, which does not substantially change later while the split peaks are forming. The second time characterizes the decay rate of the small split Kondo peak (SKP) oscillations in the conductance, which may provide a method of experimental access to it. This latter timescale is accessible via linear response from the steady state and appears to be related to the scale identified in that manner [A. Rosch, J. Kroha, and P. Wölfle, Phys. Rev. Lett. **87**, 156802 (2001)].

DOI: 10.1103/PhysRevB.71.165321 PACS number(s): 72.15.Qm, 73.50.Mx

I. INTRODUCTION

The theoretical predictions[1–3] of consequences of the Kondo effect for the steady state conduction through quantum dots began a decade ago. At low temperatures, a narrow resonance in the dot density of states can form at the Fermi level, leading to a large enhancement of the dot's conductance, which is strongly dependent on temperature, bias, and magnetic field. Many of these effects have been recently observed by a set of beautiful experiments by several groups.[4–6] These successes, supplemented by the anticipation that time dependent experiments are not far behind, have spurred a number of theoretical groups[7–12] to consider the effects expected when sinusoidal biases or gate potentials are applied. Indeed recent experiments[13] have now seen Kondo sidebands. Also the predictions[14] of split Kondo conductance peaks have been observed in double[15] and multiple[16] dots. Surprisingly, the application of steps or pulses, which can provide a less ambiguous measure of time scales than ac modulation, have been considered less extensively theoretically,[10,17,18] and not at all to our knowledge experimentally. When pulsed voltage is applied to the to the quantum dot level so that it suddenly is shifted into the Kondo regime, the conductance of the dot will begin to increase. The current saturates when the system reaches its new equilibrium configuration. In a previous investigation,[10] we considered a quantum dot biased by a small voltage and calculated the time dependent change in linear response conductance when a stepped potential was applied to a gate, thereby shifting the dot into the Kondo regime. Some general qualitative observations were made, which now can be made quantitative through the study of a different configuration of voltage switching.

In the present work we consider the response of a quantum dot, operating as a single-electron transistor, already subject to a finite dc bias when the dot level is shifted into the Kondo regime. When a finite bias is present across the dot, Kondo resonances appear at each of the leads. Due to the finite bias, these resonances are broadened in comparison with the zero bias situation.[19] While the equilibrium or zero bias situation is relatively well understood,[20] much less is know about the fully time-dependent situation, with Refs. 21 and 22 being most relevant to the present work. These two works identify two separate timescales for the quantum dot in the Kondo regime, a slow time scale[21] and a faster one.[22] The current work is a thorough study of both. While the slow time scale is also accessible through steady-state correlation functions, one needs a full dynamical theory to access the latter. Recent approaches that are complementary to the time dependent NCA used here include the determination of exact spin correlation functions at the Toulose point[23] as well as the dynamical $1/N$ approach to time-dependent currents through the dot.[24] The latter work considers the effect of pulsed bias potentials and obtains results consistent with those we previously obtained,[17] using a similar perturbation. Generalizations of this method would presumably also enable access to the faster or dynamic timescale mentioned above.

The present calculation determines, within the noncrossing approximation (NCA), the transient current after a gate pulse moves the level of the single electron transistor into the Kondo regime, under a large variety of temperatures and biases. The calculations were performed using the Kadanoff-Baym time-dependent Green function technique. The time loop Green functions of the pseudo-operators are solved in real time on a discrete grid. The transient currents are calcu-

lated directly from the current operator which can be expressed in the pseudo-operator propagators. The instantaneous spectral functions can also be calculated from the Greens functions of the pseudo operators. As mentioned above, we are able to extract two different time scales from our analysis, in addition to the trivial very rapid scale of the very small time response set by the tunneling rate to the leads (or the width of the virtual-level resonance). The first of these is characterized by the time to reach a quasimetastable point where the time-dependent conductance has essentially risen to its equilibrium value, and where the Kondo resonance has formed into a broad quasismooth structure of half-width roughly equal to the bias. The second is the time scale for the emergence and formation of the narrower individual *split* Kondo peaks (SKP), at a much slower time scale. This scale is also relevant for the decay of SKP conductance oscillations, which may provide an experimental access to it.

II. MODEL

We model the quantum dot by a single spin degenerate level of energy $\epsilon_{\rm dot}$ coupled to two leads through tunnel barriers. The Coulomb charging energy U prevents the level from being doubly occupied. The system may be described by the following Anderson Hamiltonian:

$$H(t) = \sum_{\sigma} \epsilon_{\rm dot}(t) n_{\sigma} + \sum_{k\sigma} [\epsilon_k n_{k\sigma} + (V_k c^{\dagger}_{k\sigma} c_{\sigma} + \text{h.c.})], \quad (1)$$

with the constraint that the occupation of the dot cannot exceed one electron. Here $c^{\dagger}_{\sigma}$ creates an electron of spin σ in the quantum dot, with n_{σ} the corresponding number operator; $c^{\dagger}_{k\sigma}$ creates an electron in the leads.

For zero bias across the dot, the general features of the static equilibrium spectral density when the dot level ϵ is sufficiently below the Fermi level are well known. There is a broad resonance of half-width $\Gamma(\epsilon) = 2\pi\Sigma_k |V_k|^2 \delta(\epsilon - \epsilon_k)$ at an energy $\sim \epsilon_{\rm dot}$. The notation Γ with no energy specified will always refer the value at the Fermi level. In addition, there is a sharp temperature sensitive resonance at the Fermi level (the Kondo peak), characterized by the low energy scale[25] T_K (the Kondo temperature),

$$T_K = D\left(\frac{\Gamma}{4\tilde{E}}\right)^{1/2} \exp\left(-\frac{\pi|\epsilon_{\rm dot}|}{\Gamma}\right), \quad (2)$$

where D is a high energy cutoff equal to half bandwidth when modeled by a symmetric flat band. Our calculations here use a symmetric parabolic band of half bandwidth $D_0 = 9\Gamma$. We use $D \simeq D_0/\sqrt{e}$, the choice that gives the correct normalization for the leading logarithmic corrections in the Kondo model.[26] For our case where $\epsilon_{\rm dot}$ is in the band, $\tilde{E} = D$ in Eq. (2). Only for $\epsilon_{\rm dot}$ sufficiently below the band cutoff does the form $\tilde{E} \propto |\epsilon_{\rm dot}|$, expected from the Schrieffer-Wolff transformation from the Kondo model, result. For finite bias V, the Kondo peak splits into two sub-peaks[19] at $\pm V/2$ relative to the Fermi level, which we will always take to be at zero energy. The nature of this splitting at large V has recently been elucidated.[21]

Our calculations use the noncrossing approximation (NCA), which is reliable for temperatures down to $T < T_K$.[20] The details of the time-dependent method of solution have been described in several previous publications.[26,27] Throughout this work energies, temperatures, and biases are given in units of Γ, and times in units of $1/\Gamma$, with $\hbar = k_B = e = 1$. In the regions of parameter space where T_K, T, and V are much smaller than $\epsilon_{\rm dot}$ and Γ, physical properties are functions of $T/T_K, V/T_K$, and $T_K t$, alone, provided that the quantity under consideration is made dimensionless by appropriate factors of T_K and $G_0 \equiv 2(e^2/2\pi\hbar)$. In what follows we mostly focus on properties relevant to this universal region, except when a property is directly relevant for experiments.

In the present calculations, we investigate the transient electric currents trough the dot. The current into the dot depends on the time t as

$$I_{\rm in}(t) = ie \sum_{k\sigma} V_k \langle c^{\dagger}_{k\sigma}(t) c_{\sigma}(t) \rangle + \text{c.c.} \quad (3)$$

It may be divided into contributions $I_{\rm left}(t)$ and $I_{\rm right}(t)$ by, respectively, restricting the k summations to the appropriate lead. For simplicity, we will only consider dots with left-right symmetry. The transport current is then $I(t) = 1/2[I_{\rm left}(t) - I_{\rm right}(t)]$. The finite bias on the leads is taken into account by introducing a time-dependent phase in V_k in (1). We calculate the Keldysh propagators corresponding to the angular-bracketed expectation values in (3) for each lead, and hence obtain $I(t)$.

III. TIME-DEPENDENT CONDUCTANCE RESULTS

The quantum dot systems studied in this paper all start from an equilibrium steady state with a bias across the dot equal to V. The initial value of the virtual level parameter $\epsilon_{\rm dot}(t)$ is at a negative value of magnitude sufficient that the initial Kondo temperature is much smaller than the physical temperature T. This choice of virtual level parameter ensures that the initial conductance is so small as to be negligible. In practice we use a starting value for $\epsilon_{\rm dot}(t<0) = -5\Gamma$. At $t = 0$ the virtual level parameter $\epsilon_{\rm dot}(t)$ is suddenly shifted to its final value, which we will simply call $\epsilon_{\rm dot}$ (with no time argument), with the bias V and virtual-level width parameter Γ unchanged. The majority of our calculations take $\epsilon_{\rm dot}$ to be -2Γ, and we will denote the system so described as *system one* (S1). Its Kondo temperature $T_K = 0.0022\Gamma$. We also make a number of calculations where $\epsilon_{\rm dot} = -2.225\Gamma$, for which $T_K = 0.0011\Gamma$. This latter system we call *system two* (S2).

When the dot level is in its lower position, the Kondo temperature of the dot is much smaller than the system temperature and the Kondo resonance is essentially absent. The spectral function is dominated by the broad virtual level of width $\sim 2\Gamma$ centered roughly at $\epsilon_{\rm dot}(t<0)$. When the level is moved, a new virtual-level resonance of width $\sim 2\Gamma$ is formed around the new dot level. The time scale for the formation of this resonance is Γ.[10] The Kondo resonance take longer time to form. In the $G(t)$ curves shown in this section, only this Kondo time scale is apparent.

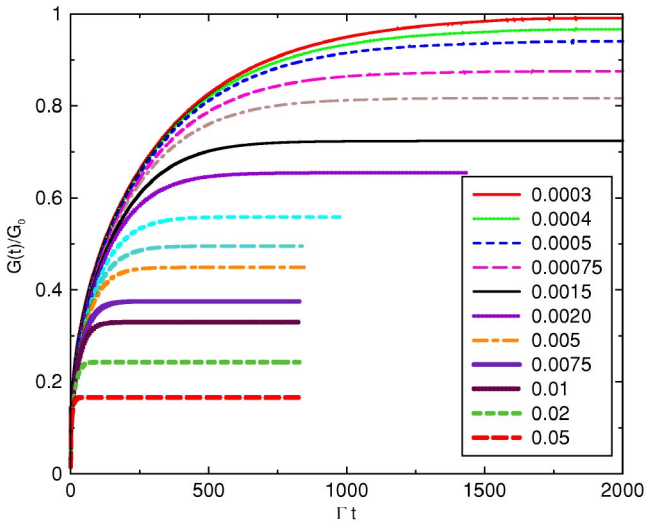

FIG. 1. (Color online) Time dependent conductance vs time for system one. The ordinate is the time dependent conductance $G(t) \equiv I(t)/V$ in units of the open-channel conductance $G_0 \equiv 2(e^2/2\pi\hbar)$. As before, $I(t)$ is the time dependent current, and V the bias. The abscissa is the time t after the gate switches the dot into the Kondo regime, in units of Γ^{-1}. The numbers in the legend are the temperatures T for the corresponding curves in units of Γ. All curves are in the linear response region of approaching zero bias V.

A. Results for small bias

We display first the results appropriate to very small V, i.e., $V \ll T_K$, such that the conductance is in the linear response regime, for a variety of temperatures in system one. These are shown in Fig. 1. It is obvious by inspection of the figure that the rise time of the conductance, whatever its precise definition should be, is increasing as the temperature is lowered. This increase begins to saturate when the temperature gets to around T_K. More quantitatively the inverse rise time (rise rate) is around T_K at low temperatures, but increases with T for higher ones. These rates are much slower than the rate Γ which is associated with the virtual level. These trends are quantified in Sec. IV.

In Fig. 2 we combine results from system one and system two to test universality. We find the results satisfying. However, we believe that the small differences between the two sets of curves are not due to computational inaccuracy, but rather are true deviations from universality, however tiny. The small time region $\Gamma t \sim 1$ is always nonuniversal, and around 25% smaller for system two than for system one. With our present algorithms, we cannot further separate the time scales using much smaller Kondo temperatures, so the results even on the Kondo time scale are still slightly affected by the nonuniversal fast contribution. For this reason, the conductances for system two will be a little smaller than for system one. In Fourier space, one could say that there is a small nonuniversal background, whose changes from system one to two are reflected in the final value of G. However, our results clearly show that the parts expected to be universal behave in this manner.

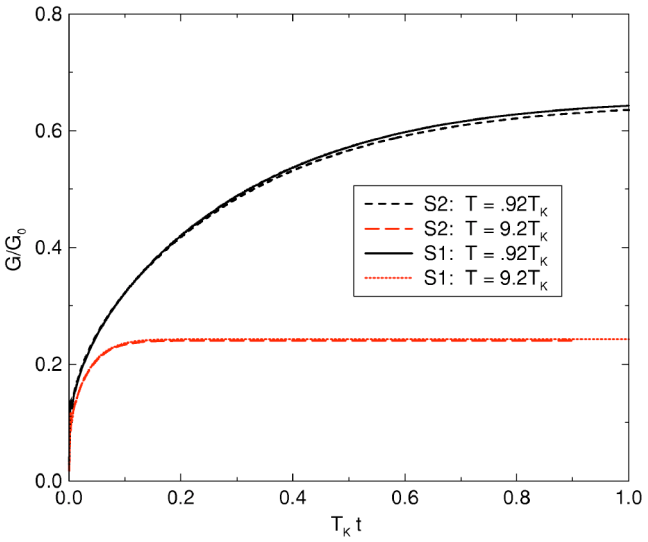

FIG. 2. (Color online) Universality of time-dependent conductance curves. The S1 curves are identical to the corresponding ones in Fig. 7 with the time axis rescaled to inverse T_K units, where here $T_K = 0.0022\Gamma$. The S2 are curves for system two (see text), which has a smaller T_K.

B. Results for finite values of bias

The finite bias calculations were performed in the same way, except that a constant bias V is present at all times. In Fig. 3 we show the results for system one for a variety of different biases and two different temperatures. The simple

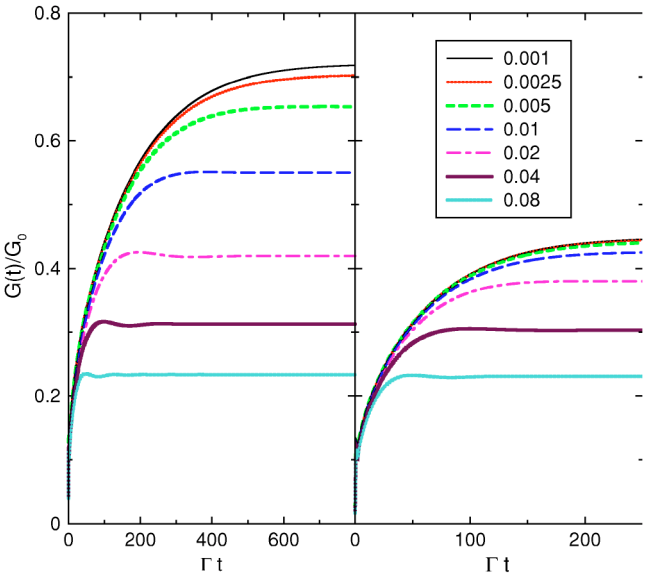

FIG. 3. (Color online) Time dependent conductance vs time. The ordinates are the time dependent conductance $G(t) \equiv I(t)/V$ in units of the open-channel conductance $G_0 \equiv 2(e^2/2\pi\hbar)$. Here $I(t)$ is the time dependent current, and V the bias. The abscissas are the time t after the gate switches the dot into the Kondo regime, in units of Γ^{-1}. Both panels are for system one (see text), with $T = 0.0015\Gamma$ (left panel) and $T = 0.005\Gamma$ (right panel). The numbers in the legend are the biases V in units of Γ for the corresponding curves in each panel.

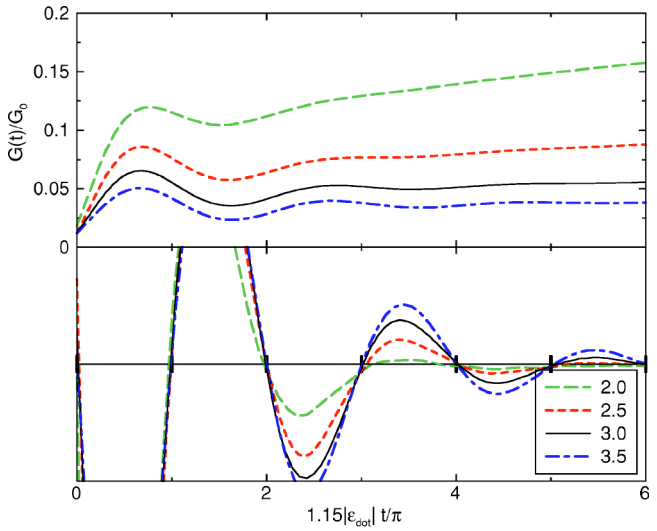

FIG. 4. (Color online) Initial oscillations at short times. The top (long-dashed) curve in the top panel is the short time version of the system one ($|\epsilon_{\rm dot}|=2\Gamma$) curve for bias $V=0.01\Gamma$. Thus it represents the very short time behavior of the curves in Fig. 3. The behavior is similar for all biases studied. The other three curves are for other values of $|\epsilon_{\rm dot}|$ whose ratio to Γ is indicated in the legend. In each case the time coordinate is rescaled as indicated, to show that the frequency of the oscillation is about equal to the magnitude of virtual resonant level's energy (measured from the Fermi level). The renormalized value of the latter is a bit larger than the bare value $|\epsilon_{\rm dot}|$. The bottom panel, showing the second derivatives of the curves in the top panel, more clearly identifies the period of oscillation.

descriptive facts that are evident by inspection of the rise-times implied by these curves are that: (i) for $V \lesssim T$ there is little change; the rising rate proportional to T discussed in the previous Sec. III A still prevails; (ii) for $V \gtrsim T$ the rising rate increases roughly linearly with V.

On a finer scale, one may see small oscillations about the final value, especially in the curves for larger V. These result from the fact[19,28] that in the presence of a finite bias V, the Kondo peak in steady state is split into two peaks at $\pm V/2$, respectively. These split Kondo peak (SKP) oscillations were clearly identified in earlier work.[17,18,29] They have a frequency almost precisely equal to V and a decay rate that is much longer than that implied by the V and T rate scales, something suggested by the prescient fact that in mean field theory the oscillations are undamped.[29] We put off a detailed analysis of this effect to a later section.

C. Initial oscillations

For small times, $\Gamma t < 10$ in Figs. 1 and 3 there appear oscillations, which are invisible on the scale of those figures. As opposed to the features mentioned in the previous two subsections, they are nonuniversal in the usual sense. However, for a given system, they take the same form and frequency, independently of T and V, at least for values of these parameters that are much smaller than $\epsilon_{\rm dot}$ or Γ. They are shown in the top curve in the top panel of Fig. 4 for system one at $T=0.0015\Gamma$ and $V=0.01\Gamma$. The next several curves show the initial oscillations for successively larger values of $|\epsilon_{\rm dot}|$. The second panel more clearly establishes that the frequency of these oscillations is the difference between the Fermi level and the virtual level position.

D. Alternative roughly equivalent measurement

The investigations described above shows that by measuring the transient currents in a quantum dot subject to a finite bias as a function of bias V and temperature, one can probe the bias-induced and thermal broadening of the nonequilibrium Kondo problem. The most straightforward implementation of such a measurement would be to measure the total charge transported through the dot $Q(\tau)$ when the dot level is subject to a pulse train in which the dot level is raised to the Kondo regime for a time τ. By measuring the total charge $Q(\tau)$ transported through the dot during a single pulse as a function of pulse length τ and taking the derivative with respect to $\tau, dQ(\tau)/d\tau$, a quantity is obtained tha/home/langreth/text/papers/nordland/qdot3/2003/PRB/resubmitt closely follows the transient currents in the dot. The equivalence would be exact if the the current were instantly returned to zero at the end of the pulse. Specifically

$$Q(\tau) = \int_0^\tau I(t)dt + \int_\tau^\infty I(t)dt. \tag{4}$$

Since the switching goes to a non-Kondo region, the dominant contribution to the turnoff rate will be $\sim\Gamma$. This means that the contribution of the second term in (4) will be small. Features that occur on that scale, like the initial oscillations, will be masked by the slightly unsharp cutoff, but the V and T rates, as well as the SKP oscillations will be preserved. In addition, the variation of $dQ(\tau)/d\tau$ will slightly lead of the variation of I, because the effective cutoff time will be slightly larger than τ. We have verified these features by explicit NCA calculations, an example of which is shown in Fig. 5.

IV. ANALYSIS AND INTERPRETATION OF ZERO BIAS RESULTS

A. Large time limit

In Fig. 6 we display the large time limit of our calculations for systems one and two. Since the bias is essentially zero, these represent the steady state linear response conductance. This figure shows that our results agree with general expectations including approximate universality.

The exact asymptotic curve at large $\ln(T/T_K)$

$$\frac{G}{G_0} = \frac{3\pi^2}{16\ln^2(T/T_K)} \tag{5}$$

was first calculated by Abrikosov[30] for the Kondo impurity problem, and has been more recently adapted and applied to quantum dots.[31] It can also be derived by the so-called poor man's scaling method.[32,33] However, if one applies the perturbative procedure used in Ref. 21 for large V to the similar large T case, one finds that within NCA, the asymptote is $4/3$ times the value in Eq. (5) The NCA asymptote is the one

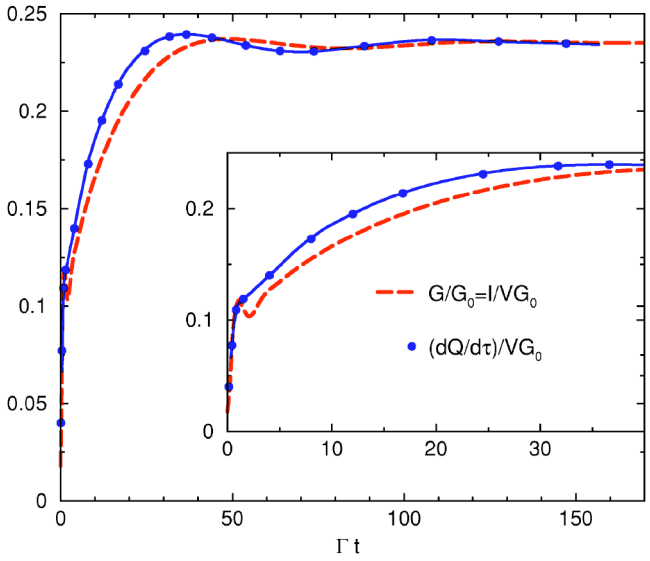

FIG. 5. (Color online) Comparison of instantaneous conductance $G(\tau)=I(\tau)/V$ as a function of time τ after the level was moved and $[dQ(\tau)/d\tau]/V$ as a function of pulse length τ, both expressed in units of G_0. The quantum dot is system one. The bias across the dot is $V=0.08\Gamma$ and the temperature is $T=0.0015\Gamma$.

shown in the figure. Our lowest temperature point (not shown) is slightly above the unitarity limit, another NCA error also found by others.[21]

B. Extraction of the rise rate

Here we use previous analytic results[10] to extract the rise time τ from the data of Fig. 1. What was found there, was that the current response to a stepped turning on of the Kondo interaction would be the same as the *equilibrium* response to a time-dependent *effective temperature* T_e given by $T_e=T\coth \pi Tt/2\hbar$. We start with the tautology $\delta I/I=[d(\ln G)/d(\ln T_e)]\delta T_e/T_e$ Defining the fraction f as the finite difference

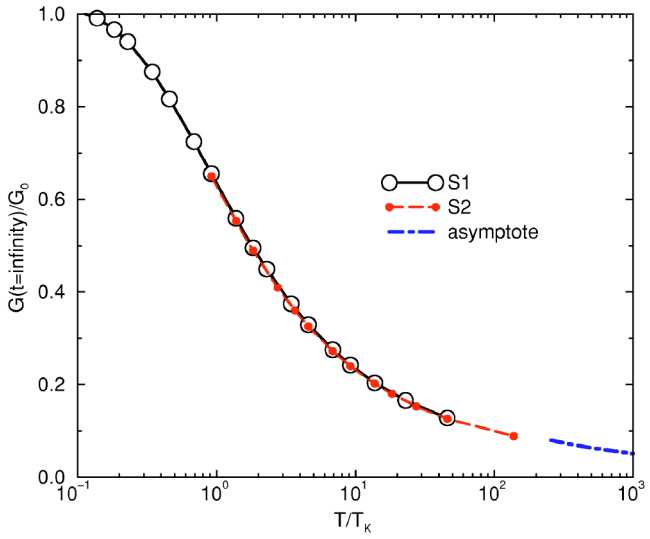

FIG. 6. (Color online) The large-time limit of $G(t)/G_0$ vs temperature. Since $V\sim 0$, this is the equilibrium value of G/G_0. The points labeled S1 and S2 are from system one and two, respectively (see text). The curve labeled *asymptote* in the legend represents the large T asymptote within NCA (see text).

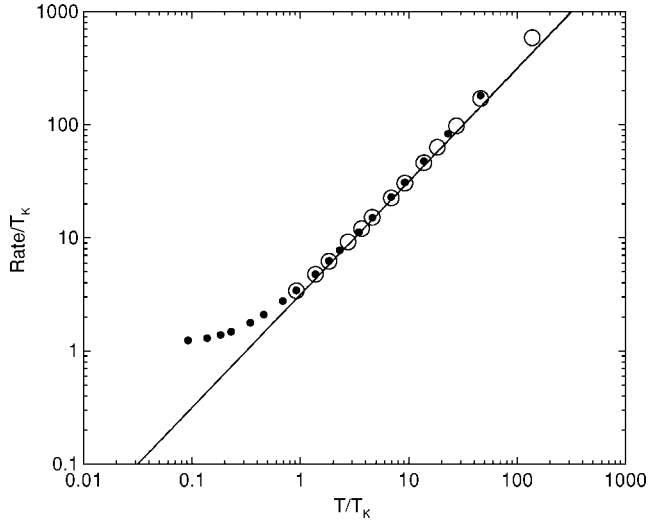

FIG. 7. Rate $(1/\tau)$ at which the conductance approaches its final value vs temperature T, with zero bias $V=0$. The solid dots are for system one (see text), while the open circles are for system two, which has a different Kondo temperature T_K. The solid curve is a straight line of slope π through the origin [see Eq. (9)].

$$f \equiv \frac{I(\infty)-I(t)}{I(\infty)}, \tag{6}$$

and

$$f_0 \equiv -2\frac{d(\ln G)}{d(\ln T)}, \tag{7}$$

we have in the large t limit $f\to f_0(\coth \pi Tt/2\hbar-1)/2$. which becomes

$$f \to f_0 \exp\left(-\frac{t}{\tau}\right), \tag{8}$$

with

$$\frac{1}{\tau} = \pi T. \tag{9}$$

This suggests that we should fit the upper part of the our curves in Fig. 1 to Eq. (8), and compare the resulting τ with Eq. (9). Since the derivation in Ref. 10 was only to lowest logarithmic order (and certainly cannot be expected to be valid for $T\lesssim T_K$), there exists a possibility of logarithms of T/T_K to become predominant at large T. However, we find no evidence for the latter effect in the curves of Fig. 1. We display the rates $(\equiv 1/\tau)$ that we find in Fig. 7. The quite good agreement of the curves in Fig. 7 over a major part of the range is satisfying. The curves also strongly suggest that the low temperature limit of Eq. (9) replaces T by something of the order of T_K. Our points appear to deviate slightly from Eq. (9) at higher temperatures. However, our fitting procedure is less accurate at high temperatures where $G(\infty)$ is

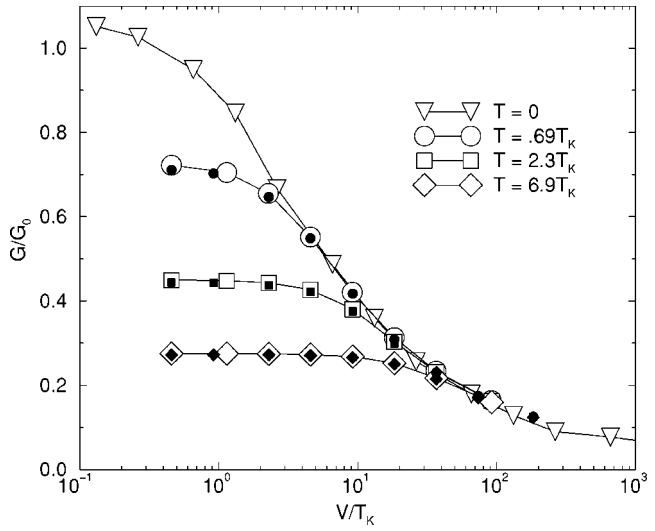

FIG. 8. Long time or dc conductance vs bias. The ordinate G/G_0 is the dc conductance in units of the open channel conductance $G_0=2e^2/2\pi\hbar$ for the two spins, while the abscissa is the bias V in units of the Kondo temperature T_K. The triangles represent the zero temperature NCA data of Ref. 21 with the abcissa rescaled to correct for the ~30% difference between the two definitions of the Kondo temperature. The open circles, squares, and diamonds represent the long time saturation of our time-dependent conductance curves for system one at the temperatures indicated. The smaller solid symbols represent the values at the same respective temperatures for system two, which is a different Kondo temperature (see text).

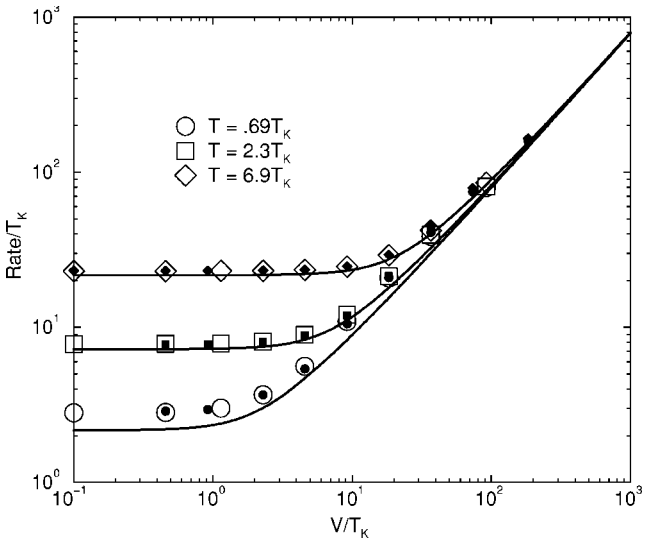

FIG. 9. Rate (inverse time) at which the conductance approaches its "final value" vs bias V, at several temperatures as indicated. The open circles, squares, and diamonds are for system one (see text), while the corresponding solid symbols are for system 2, which has a different Kondo temperature. Our $V=0$ points are shown in the figure at $V/T_K=0.1$. The solid lines are the predictions of Eq. (10).

small, and our estimated numerical error is of the same magnitude as this deviation. For this reason, we are not prepared to say with certainty whether the slight deviation of our calculated rates from Eq. (9) at large temperatures is a real effect or not.

An analysis of the temporal evolution of the instantaneous spectral function of the dot level does reveal significant spectral reshaping of the Kondo resonance well beyond the time where the conductance has saturated.[10] This effect suggests the presence of a slower time scale at large temperatures. We might certainly expect a slower timescale to emerge, if we apply the arguments of Ref. 21 to the low bias, high temperature case, as done in Appendix A. A more detailed investigation of the origin of this effect and the possibility for its experimental detection is in progress. Experimentally this will be more difficult than the large V case discussed later, because here the Kondo peak is not split, so there are no oscillations originating from that source. At the moment the computational effort required prevents further numerical results from being presented here.

V. ANALYSIS AND INTERPRETATION OF FINITE BIAS RESULTS

A. Large time limit

We begin by plotting the large time values of $G(t)$ in our finite V calculations. This quantity is the steady state conductance, and our curves in Fig. 8 supplement results previously calculated[21] for $T=0$, which are included in the plot. Since the formula for the Kondo temperature used there gave a value some 30% greater than Eq. (2), their values for V/T_K were rescaled appropriately, so they could be put on the same graph with ours. Our values show approximate universality as discussed earlier and agreement with Ref. 21 in the appropriate regions.

B. Extraction of the rise rate

The very large time behavior of our curves in Fig. 3 is dominated by the decay of the SKP oscillations. It is clear that their amplitude is very small and for the smaller V's entirely negligible. Since the amplitude of the SKP oscillations is small, they will have no effect on any common sense definition or experimental measurement of the risetime. Despite the SKP oscillations, the form Eq. (8) well describes the upper part of the time-dependent conductance curves in Fig. 3 up until they reach within ~1% of the saturation value. Therefore, as a practical empirical technique to characterize the rise time, we use the same technique as for $V=0$. The results of this analysis are shown in Fig. 9.

C. Interpretation

If the physical origin of the T dependence in Eq. (9) is the same as the source of the T dependence in the Korringa rate, Eq. (A1), then it arises because a change in **S** involves the absorption of an electron-hole pair of zero energy from the leads. The phase space for such a process is doubly restricted by the Pauli principle, and produces the factor $\int d\epsilon\, f(\epsilon)(1-f(\epsilon))=T$ where $f(\epsilon)$ is the Fermi function.

The application of these ideas to a biased dot allows the phase space factor to be tuned in a continuous fashion by

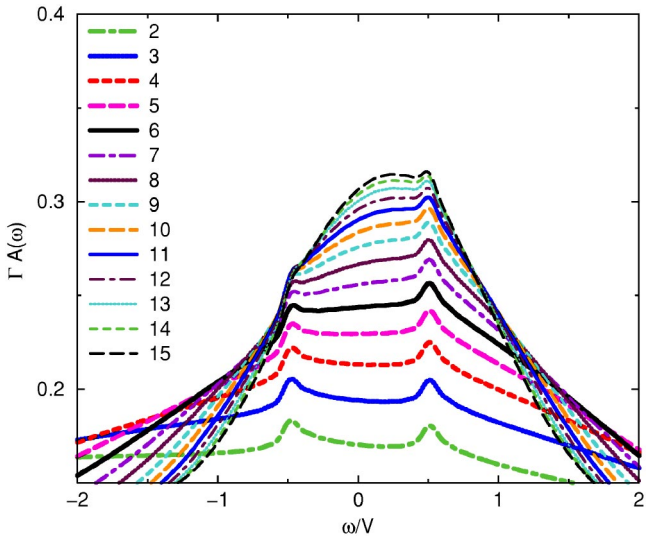

FIG. 10. (Color online) Time-dependent spectral functions for the time scale relevant for the rise time of the conductance. These curves are for system one with $T=0.0015\Gamma=0.69T_K$, and $V=0.08\Gamma=37T_K$. The curves are at equal time intervals $\Delta t=2.8\Gamma^{-1}=0.006T_K^{-1}=0.17(4/\pi V)$, where the $4/\pi V$ factor is motivated by the high temperature asymptote of Eq. (10). This factor has the value of unity at $t=6\ \Delta t$ (thick solid black curve). The lowest curve is for time $(t=2\ \Delta t)$ after the virtual level parameter was switched to its final value of -2Γ. By curve 15 the conductance has for all practical purposes reached its dc value.

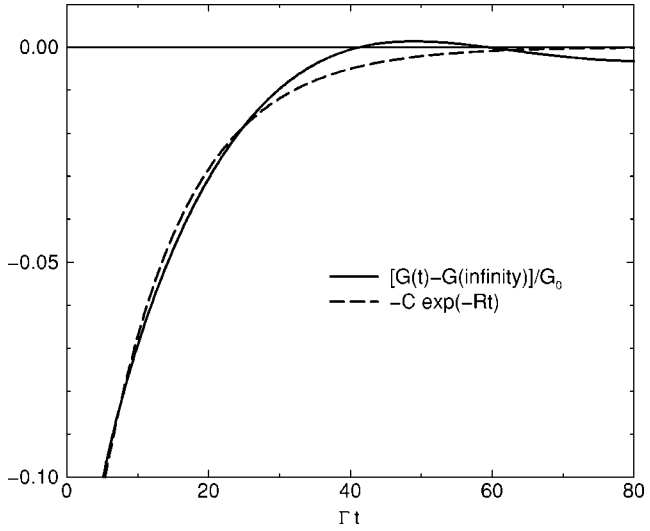

FIG. 11. The rise in conductance as the Kondo peak forms for bias $V=0.08\Gamma$ at $T=0.0015$. The solid curve is a magnified section of the corresponding curve in Fig. 3 with the horizontal axis shifted as indicated in the legend. The dashed curve is the indicated exponential fit. The rate R obtained in this way characterizes the risetime $(R=1/\tau)$ of the conductance, and this is the rate used in the preparation of Fig. 9. Of all the curves in Fig. 3 this is the worst case for the exponential fit, because here the SKP oscillations are largest. The first period of these oscillations is partially visible here. Multiple cycles are shown in the larger magnification of Fig. 13. The quantum dot is system one.

varying the bias V across the two leads of the dot, which for simplicity we assume to be symmetric under lead interchange. The phase space restriction factor in this case is given by $\frac{1}{4}\Sigma_{l,l'}\int d\epsilon\, f_l(\epsilon)(1-f_{l'}(\epsilon))$, where the indices l and l' designate which lead is referred to. For example, the Fermi functions $f_1(\epsilon)$ and $f_2(\epsilon)$ have Fermi levels displaced by $\pm eV/2$, respectively, where e is the magnitude of the electronic charge and V is the bias. The integral above can be evaluated analytically, with the result that Eq. (9) should be replaced by

$$\frac{1}{\tau}=\pi TF\left(\frac{V}{T}\right), \tag{10}$$

where

$$F(x)=\frac{1}{4}\left(1+1+\frac{x}{1-e^{-x}}+\frac{xe^{-x}}{1-e^{-x}}\right). \tag{11}$$

In writing Eq. (11) we have sacrificed conciseness to facilitate clarification of the origin of the terms in parentheses, in terms of the wave function of the annihilated particle-hole pair. The first two terms arise when the two components of this object are in the same lead; in this case the existence of V has no effect on the result; the phase space for these processes is still constricted, and the contribution to $1/\tau$ is still small. For the third term, the particle is on lead 1 and the hole on lead 2; here the phase space is opened wide by V. Finally for the fourth term, the particle is on lead 2 and the hole on lead 1; the phase space is, aside from an exponentially small tail, closed off entirely as V is increased. So the essential physical feature deriving from Eq. (11) is that the factor of T in Eq. (9) is replaced at large V by $\frac{1}{4}V$. The notion of an expanded phase space is implicit in the Anderson model rate calculation of Wingreen and Meir[19] and in a different context in the work of Kaminski *et al.*[12] In any case, the rate of Eq. (10) provides a way to rationalize the calculated points in Fig. 9 in a parameter free way, which has predictive power for the rise-time of the conductance. The comparison shown in that figure shows that it captures the main trends of the NCA results, although not with such good agreement as for the $V=0$ case (Fig. 7).

VI. TIME-DEPENDENT SPECTRAL FUNCTION: TWO TIME SCALES

A. Faster time scale

As an aid to the interpretation of the conductance behavior, we display the time-dependent spectral functions $A_{\rm dot}(\omega,t)$ for the dot.[31] Figure 10 shows the case $T=0.0015\Gamma=0.69T_K$ and $V=0.08\Gamma=37T_K$. The snapshots shown here are for the time scale appropriate for the risetime of of the conductance, as shown in detail in Fig. 11. Figure 10 shows the rise of the Kondo peak as a mostly smooth structure of half-width $\sim V$, with the individual split peaks mostly undeveloped. This structure appears to be converging toward a quasistationary steady state. It is clear that this time scale, intermediate between the trivial very rapid time scale governed by the Γ rate, and the longest time scale yet to emerge, is the one governing the risetime of the conductance.

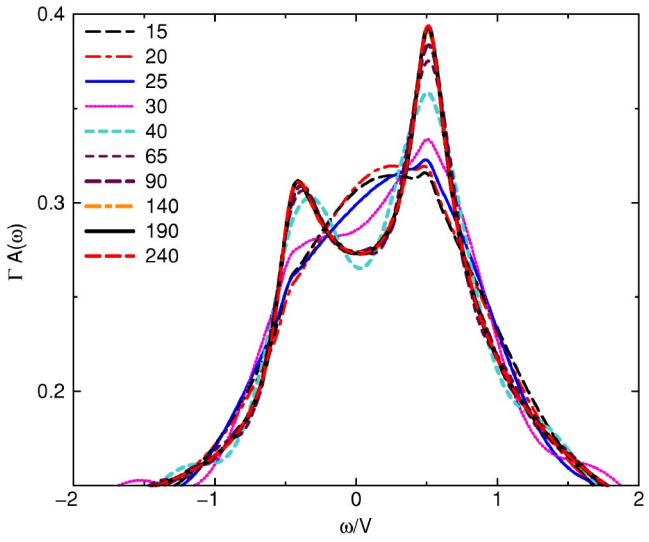

FIG. 12. (Color online) Time-dependent spectral functions for the time scale relevant for the development of the split Kondo peak and the damping of SKP oscillations. This is a continuation of the snapshots shown in Fig. 10, so all the parameters have the values shown in the caption of that figure. Here, however, the time interval between the successive snapshots is much greater, varying from 5 Δt to 50 Δt, as indicated by the labeling in the legend. The quantum dot is system one.

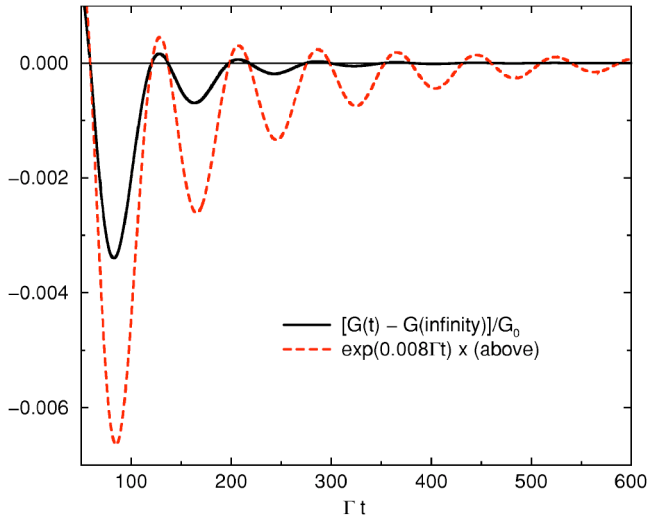

FIG. 13. (Color online) SKP oscillations for bias $V=0.08\Gamma$ at $T=0.0015$. The solid curve is a magnified section of the corresponding curve in Fig. 3 with the position of the horizontal axis shifted as indicated in the legend. The dashed curve is a progressively more magnified version of the solid curve, so that more SKP oscillations can be seen. As indicated in Fig. 15, the angular frequency of these oscillations is almost exactly equal to V. The quantum dot is system one.

It is probably only available through a fully nonequilibrium theory, since it is the scale relevant for approaching a steady state that is metastable at best. It is therefore probably unavailable through perturbation theory from the true steady state, and hence will not likely appear in steady-state correlation functions.

B. Slower time scale

Figure 12 shows the development of the spectral function on the longest time scale, showing the rate at which the individual split peaks emerge from the quasistructure of width V formed at the metastable point. For $V \gg T_K$, this latter rate is much smaller than that illustrated in Fig. 10, in this case by an order of magnitude. During the time interval shown in Fig. 12, the conductance changes only by the small oscillatory amounts indicated by the SKP oscillations. Indeed, in this time interval, the area under A_{dot} (when $T \ll V$) in between $-V/2$ and $V/2$ remains almost constant in time, with the additional area under the split peaks being almost exactly compensated by the loss in area between peaks. We have verified that the conductance in this regime, which still has a tiny fluctuation due to the SKP oscillations, is given by the steady-state formula [for example, Eq. (12) of Ref. 19], provided that the A_{dot} used is the time-dependent instantaneous spectral function.[34]

VII. SKP OSCILLATIONS AND THE LONGEST TIME SCALE

A. SKP oscillations in the quantum dot

In Fig. 11, which extends a little beyond the range of Fig. 10, one can see the beginnings of the SKP oscillations. The continuations of them on a highly magnified scale are shown in Fig. 13. Generally, many complete periods of oscillation can be seen, and this period corresponds almost exactly to an angular frequency of V, becoming closer and closer from below as V gets larger and larger. The details of this analysis is given in Appendix B. There it is also shown that the decay rate is close to constant (exponential decay). For large V this rate is substantially smaller than the rates identified earlier characterizing the risetime of the conductance. The method of extraction of the rates is described in Appendix B.

For the case shown here, the decay rate of the SKP oscillations is on the order of the distance to the inflection point on either of the peaks in the converged spectral function.[35] The rate is not inconsistent with, but possibly a little slower than, the slow-scale rise rate of the time dependent spectral function, although the latter is more difficult to pinpoint. We can with much less ambiguity compare this rate with the 2γ rate identified in Ref. 21, and calculated for $T=0$; γ was defined to be the the imaginary part of the pseudofermion self-energy.

What we find is that if we divide the SKP oscillation decay rates by two, then these values at our lowest temperature ($\sim 0.3T_K$) agree within their accuracy with the 2γ curve. This is shown in Fig. 14. We are not certain why half the decay rate is what seems to correspond to 2γ but presumably the issue is dephasing which occurs both at $-V/2$ and $+V/2$ giving roughly additive contributions. Another possibility is that $T=0$ (which is currently unavailable for us) will be further from our lowest points at $T=0.34T_K$ than we expect. But a definitive answer will have to await further and more complete studies. What is very clear, however, is that the damping of SKP oscillations is controlled by a rate much slower than $\sim V$ for large V, and which is numerically quite close to the 2γ rate.

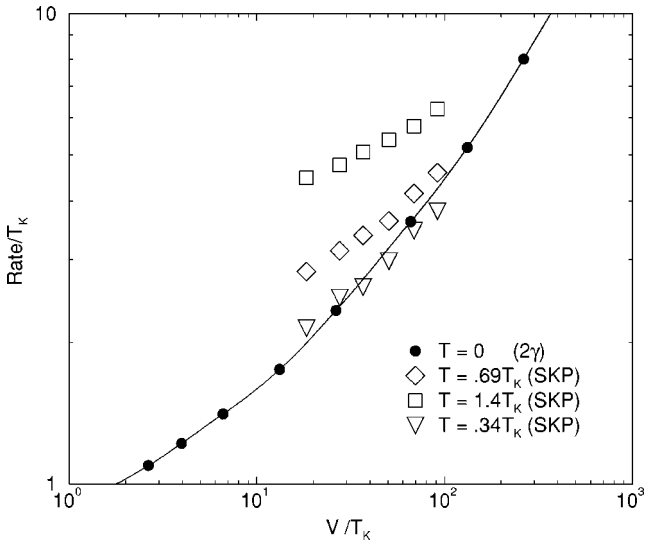

FIG. 14. Decay of SKP oscillations vs bias V. The empty squares, diamonds, and triangles represent data derived from the damping rate of the SKP oscillations in our calculations of conductance vs time at the temperature indicated, respectively. The quantum dot is system one. The solid circles are the calculations of 2γ at zero temperature in Ref. 21.

B. Decay of SKP oscillations in N-fold degenerate models

We conclude this section by discussing models with larger degeneracy N than the $N=2$ appropriate for quantum dots. Repeating the large V NCA perturbative analysis[21] for that case gives

$$2\gamma = \frac{\pi V}{2N \ln^2 \frac{V}{T_K}}. \tag{12}$$

As noted in Appendix A, the NCA *does not* need correcting by multiplying this by $S(S+1)$, which would be proportional to N^2 at large N. Equation (12) indicates that the decay rate of SKP oscillations approaches zero as $1/N$ for large N. This is consistent with the trend of NCA studies[36] of this damping as a function of N, and with the fact[29] that these oscillations are undamped in mean field theory ($N=\infty$). In this case the effect of the vertex correction (see Appendix A) is dramatic indeed, making a qualitative change, as opposed to the $\sim$30% correction for the $N=2$ quantum dot case.

VIII. ADDITIONAL CONCLUSIONS

Many of our important conclusions are contained in the abstract and final paragraph of the introduction. We mention here the few that are not.

First, for $V\sim 0$ the risetime of the conductance is very accurately characterized by the simple expression $1/\tau = \pi T$, Eq. (9), over a wide range of temperature $T > T_K$, and appears to heal towards T_K for smaller T. Second, for $V > \sim 4T$, one should replace T by $V/4$ in the above. These rates appear to lead toward a quasimetastable point, and do not negate the emergence of slower rates at longer times, which in the case of larger V control the damping of SKP oscillations. Third, at the very beginning of switching the gate, there are small initial nonuniversal oscillations at a frequency corresponding to the dot level's separation from the Fermi level (for V's small with respect to that separation). Finally we predict for N-fold degenerate models, that the damping of SKP oscillations decreases as $1/N$ for $V \gg T_K$.

Although our calculations are framed in terms of the Anderson model, through universality and the Schrieffer-Wolff transformation, we are really dealing only with the issue of the decay of excitations produced by switching the Kondo temperature T_K from far below the physical temperature to something that is much less below or comparable to T_K. This means that any change in the physical parameters that have the same effect on T_K (and no other effect) will produce the same physical effects. The ability to observe the long time scale will of course be independent of excitation method (one only needs to wait long enough), and nonuniversal methods such as sudden switching from a mixed valent state could be used. However, the ability to observe the the faster time scale under such nonuniversal excitation methods must be regarded as unknown, pending further study.

ACKNOWLEDGMENTS

We thank A. Rosch for relevant communications. The work was supported in part by NSF Grants No. DMR 97-08499 and DMR 00-93079 (Rutgers University), and the Robert A. Welch Foundation under Grant No. C-1222 (Rice University).

APPENDIX A: THE KORRINGA RATE

A half a century ago, the framework and starting point for discussion of the time scale τ for a localized spin in an electron sea was set by Korringa,[37] whose contribution has been promulgated at the textbook level for decades.[38] In simple terms $1/\tau$ gives the fractional rate at which a component of spin $\mathbf{S}$ representing a magnetic impurity (or a quantum dot) is changing due to the electrons in the conduction band (or in the leads of a quantum dot). It is given by an expression of the type

$$\frac{1}{\tau_{\mathrm{kor}}} = \alpha T, \tag{A1}$$

where α is a dimensionless constant and T is the temperature. Although Korringa's original derivation applied to a nuclear spin where the interaction with electrons is dipolar, it has been widely applied to impurity electron spins as well, using the Kondo model

$$H = \sum_i (\epsilon_{k_i} - J\mathbf{s}_i \cdot \mathbf{S}), \tag{A2}$$

for the interaction. In Eq. (A2), k_i is a generalized quantum number for the ith conduction (or lead) electron, ϵ_{k_i} is its energy, and $\mathbf{s}_i$ is its spin operator. For a symmetric quantum dot, k is assumed to include the information on which lead is referred to. The exchange coupling J is taken to be independent of k, aside from the usual high-energy cutoff at energies

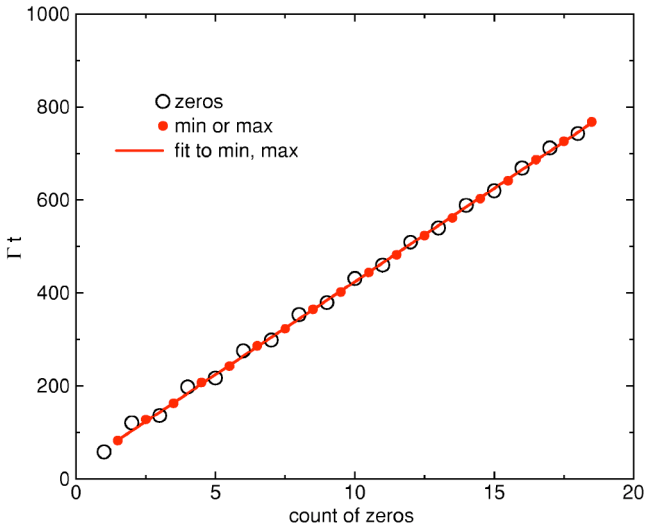

FIG. 15. (Color online) Positions of extrema and zeros of SKP oscillations for $V=0.080\Gamma$ as in Fig. 13. The slope of the fitted line gives a frequency of 0.0783Γ. The frequency is always slightly less than V, but for our largest V's, we find the difference to be only around 0.1%. The quantum dot is system one.

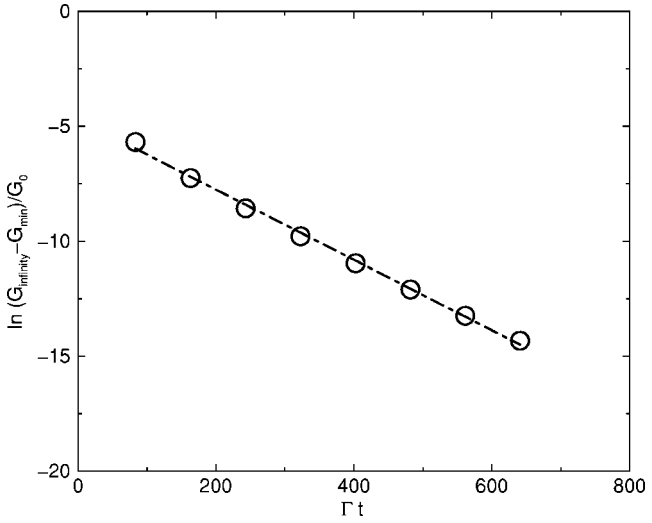

FIG. 16. Determination of the decay rate of the SKP oscillations from the positions of the minima in Fig. 13. The slope of the curve gives a rate of 0.015Γ for $V=0.08\Gamma$ and $T=0.0015$. These rates are universal functions of V/T_K and T/T_K, and hence depend on Γ, E, and D only through Eq. (2). The quantum dot is system one with a Kondo temperature $T_K=0.0022\Gamma$.

further than D above or below the Fermi level. In terms of Anderson model parameters $J=-2|V|^2/\epsilon_{\rm dot}$, where here V is the matrix element in Eq. (1), and not the bias voltage. To lowest order in J, the quantity α in Eq. (A1) is given, for example, by Eq. (1.16) in Ref. 39,

$$\alpha = \pi(J\rho)^2, \tag{A3}$$

where ρ is the density of states in the leads (both leads together), when applied to a symmetric quantum dot.

One should note that (A3) applies to a general spin (S) Kondo model, ($S=\frac{1}{2}$ for a quantum dot), and *there is no factor of* $S(S+1)$. For $S=\frac{1}{2}$ this can be shown to be incontrovertible by the solution of a simple master equation for the occupation probability of up or down spin states $\dot{P}_\sigma = -R(P_\sigma - P_{-\sigma})$, where $R=R_{\uparrow\downarrow}=R_{\downarrow\uparrow}$ is the spin-flip rate of the dot spin due to its interaction with the lead electrons. This is readily solved for the decay rate of an averaged spin component $\langle \dot{S}_m\rangle = -\langle \dot{S}_m\rangle/\tau_{\rm kor}$ where $1/\tau_{\rm kor}=2R=\alpha T$, where $R_{\downarrow\uparrow}$ was evaluated by the Fermi golden rule, giving (A1) with α given by (A3).

While it is true that the equilibrium pseudo-fermion propagator's self-energy's imaginary part *does* indeed contain the $S(S+1)$ factor [Eq. (C4) in Ref. 39], the time decay rate of the spin correlator does not, because of vertex corrections, which are summed in Ref. 39 via the Kadanoff-Baym equations.

When J is rescaled via the poor man's scaling technique, $J\rho \to -1/\ln(T/T_{\rm K})$, as done by many authors to obtain results valid for $\ln(T/T_{\rm K}) \gg 1$, one gets

$$\frac{1}{\tau} = \frac{\pi T}{\ln^2 \frac{T}{T_{\rm K}}}. \tag{A4}$$

Similarly one gets large V results through the replacement $T \to \frac{1}{4}V$ in Eq. (A4). These agree exactly with what one gets from high V or high T expansions[21] of the NCA equations, and we conclude that NCA gets the right answer here. Of course, the NCA misses the factor $\frac{3}{4}$ in the conductance, Eq. (5), as previously pointed out.[21]

APPENDIX B: DETAILS OF SKP OSCILLATION PARAMETERS

In Fig. 15 we map the successive positions of the zero crossings as well as the positions of the maxima an minima for the case shown in Fig. 13. It is obvious that a fixed period is maintained over many cycles. This period is determined by a least squares fit to the minimum and maximum positions. The zero crossings straddle the fitted line because the peak-to-peak envelope center is still a small way below its final value. The decay rate was determined as shown in Fig. 16, by a least square fit to the logarithm of the difference between the dc conductance and its value at the minimum points vs. the time corresponding to these points. If one looks closely, there appears to be a small curvature at the beginning. This is probably real and not noise, as according to Fig. 12, the split Kondo peaks in the instantaneous spectral functions are still narrowing slightly in this region. Aside from rejecting early points that were obviously out of line, we did not attempt to account for this in the analysis. The small misalignment of the final point, on the other hand is certainly due to noise, an ubiquitous feature for extremely large times, which deterred us from trying to distinguish between the "initial" and "final" slopes.

[1] T. K. Ng and P. A. Lee, Phys. Rev. Lett. **61**, 1768 (1988).
[2] L. I. Glazman and M. E. Raikh, JETP Lett. **47**, 452 (1988).
[3] S. Hershfield, J. H. Davies, and J. W. Wilkins, Phys. Rev. Lett. **67**, 3720 (1991).
[4] D. Goldhaber-Gordon, H. Shtrikman, D. Mahalu, D. Abusch-magder, U. Meirav, and M. A. Kastner, Nature (London) **391**, 156 (1998).
[5] D. Goldhaber-Gordon, J. Gores, M. A. Kastner, H. Shtrikman, D. Mahalu, and U. Meirav, Phys. Rev. Lett. **81**, 5225 (1998).
[6] S. M. Cronenwett, T. H. Osterkamp, and L. P. Kouwenhoven, Science **281**, 540 (1998).
[7] M. H. Hettler and H. Schoeller, Phys. Rev. Lett. **74**, 4907 (1995).
[8] A. Schiller and S. Hershfield, Phys. Rev. Lett. **77**, 1821 (1996).
[9] T. K. Ng, Phys. Rev. Lett. **76**, 487 (1996).
[10] P. Nordlander, M. Pustilnik, Y. Meir, N. S. Wingreen, and D. C. Langreth, Phys. Rev. Lett. **83**, 808 (1999).
[11] Y. Goldin and Y. Avishai, Phys. Rev. Lett. **81**, 5394 (1998).
[12] A. Kaminski, Y. V. Nazarov, and L. I. Glazman, Phys. Rev. Lett. **83**, 384 (1999).
[13] A. Kogan, S. Amasha, and M. A. Kastner, Science **304**, 1293 (2004).
[14] R. Aguado and D. C. Langreth, Phys. Rev. Lett. **85**, 1946 (2000); Phys. Rev. B **67**, 245307 (2003).
[15] H. Jeong *et al.*, Science **293**, 2220 (2001).
[16] N. J. Craig *et al.*, Science **304**, 565 (2004).
[17] M. Plihal, D. C. Langreth, and P. Nordlander, Phys. Rev. B **61**, R13 341 (2000).
[18] A. Schiller and S. Hershfield, Phys. Rev. B **62**, R16 271 (2000).
[19] N. S. Wingreen and Y. Meir, Phys. Rev. B **49**, 11 040 (1994).
[20] N. E. Bickers, Rev. Mod. Phys. **59**, 845 (1987).
[21] A. Rosch, J. Kroha, and P. Wölfle, Phys. Rev. Lett. **87**, 156802 (2001).
[22] M. Plihal, D. C. Langreth, and P. Nordlander, cond-mat/0108525 (unpublished).
[23] D. Lobaskin and S. Kehrein, cond-mat/0405193 (unpublished).
[24] J. Merino and J. B. Marston, Phys. Rev. B **69**, 115304 (2004).
[25] For example, see A. C. Hewson, *The Kondo Problem to Heavy Fermions* (Cambridge UP, Cambridge, 1993). In consistency with the practice in quantum dot physics, we use the notation T_K in such a way that if one replaces T by T_K in the Curie law, the known Bethe ansatz result for the susceptibility at $T=0$ is obtained, while Hewson uses the T_K defined from the high T expansion. The latter, through inclusion of the Wilson number, would yield a value around 40% as big. However, in the preliminary version of a piece of this work (cond-mat/0108525), this smaller value was used, thus explaining the apparent disagreement between that work and this.
[26] H. Shao, D. C. Langreth, and P. Nordlander, Phys. Rev. B **49**, 13 929 (1994).
[27] D. C. Langreth and P. Nordlander, Phys. Rev. B **43**, 2541 (1991).
[28] N. Sivan and N. S. Wingreen, Phys. Rev. B **54**, 11 622 (1996).
[29] P. Coleman *et al.*, J. Phys.: Condens. Matter **14**, L205 (2002).
[30] A. A. Abrikosov, Physics (Long Island City, N.Y.) **2**, 5 (1965).
[31] P. Nordlander, N. S. Wingreen, Y. Meir, and D. C. Langreth, Phys. Rev. B **61**, 2146 (2001).
[32] P. W. Anderson, J. Phys. C **3**, 2439 (1970).
[33] A. Kaminski, Y. V. Nazarov, and L. I. Glazman, Phys. Rev. B **62**, 8154 (2000).
[34] Since n_{dot} is a virtual constant, this follows from the discussion around Eq. 25 in A.-P Jauho, N. S. Wingreen, and Y. Meir, Phys. Rev. B **50**, 5528 (1994).
[35] One can show that for large $\ln(V/T_K)$, the width of each of the split Kondo peaks in the steady-state spectral function, as measured between the inflection points, is the 2γ defined in Ref. 21. To do this one must consider the additional rounding mentioned there, but not included in their Eq. (3). This width is of course much smaller than the width at half maximum.
[36] M. Plihal and D. C. Langreth (unpublished).
[37] J. Korringa, Physica (Amsterdam) **16**, 601 (1950).
[38] C. P. Slichter, *Principles of Magnetic Resonance* (Springer, Berlin, 1990).
[39] D. C. Langreth and J. W. Wilkins, Phys. Rev. B **6**, 3189 (1972).